



HAL
open science

Rotational Fingerprints of Vinylketene for Astronomical Observations

L. Kolesnikova, T. Uhlíkova, J. Koucký, K. Luková, D. Habiger, P. Kania,
Jean-Claude Guillemin, I. Urban

► **To cite this version:**

L. Kolesnikova, T. Uhlíkova, J. Koucký, K. Luková, D. Habiger, et al.. Rotational Fingerprints of Vinylketene for Astronomical Observations. *The Astrophysical Journal*, 2023, 944 (1), pp.10. 10.3847/1538-4357/acade3 . hal-04019025

HAL Id: hal-04019025

<https://hal.science/hal-04019025>

Submitted on 30 May 2023

HAL is a multi-disciplinary open access archive for the deposit and dissemination of scientific research documents, whether they are published or not. The documents may come from teaching and research institutions in France or abroad, or from public or private research centers.

L'archive ouverte pluridisciplinaire **HAL**, est destinée au dépôt et à la diffusion de documents scientifiques de niveau recherche, publiés ou non, émanant des établissements d'enseignement et de recherche français ou étrangers, des laboratoires publics ou privés.



Distributed under a Creative Commons Attribution 4.0 International License



Rotational Fingerprints of Vinylketene for Astronomical Observations

Lucie Kolesníková¹ , Tereza Uhlíková¹ , Jan Koucký¹ , Kateřina Luková¹ , Dominik Habiger¹, Patrik Kania¹ ,
Jean-Claude Guillemin² , and Štěpán Urban¹

¹Department of Analytical Chemistry, University of Chemistry and Technology, Technická 5, 166 28 Prague 6, Czech Republic; lucie.kolesnikova@vscht.cz

²Univ Rennes, Ecole Nationale Supérieure de Chimie de Rennes, CNRS, ISCR UMR6226, F-35000 Rennes, France

Received 2022 September 5; revised 2022 November 2; accepted 2022 November 6; published 2023 February 8

Abstract

A high degree of isomerism in the realm of interstellar molecules stimulates systematic astronomical investigations of members of different families of isomers. Among them, vinyl-bearing compounds have kindled considerable interest due to recent detections of vinylamine, vinylacetylene, and vinylcyanoacetylene. Herein, we open the possibility to search for vinylketene in the interstellar space by means of its rotational transitions. The pure rotational spectrum of the title molecule was recorded in the frequency regions 195–218 and 293–324 GHz and an improved and extended set of spectroscopic parameters has been obtained for the most stable *trans* conformer. In addition, rotational signatures and molecular constants for the less stable *cis* form are reported for the first time. We provide a catalog of precise transition frequencies and intensities of vinylketene to the astronomical community and pave the way toward interstellar explorations of C₄H₄O isomer family.

Unified Astronomy Thesaurus concepts: [Catalogs \(205\)](#); [Molecular spectroscopy \(2095\)](#); [Interstellar molecules \(849\)](#); [Laboratory astrophysics \(2004\)](#); [Experimental data \(2371\)](#)

Supporting material: machine-readable tables

1. Introduction

A considerable activity has been noticed in recent years concerning the astronomical investigations of vinyl (C₂H₃–) containing species in the interstellar medium (ISM; Molpeceres & Rivilla 2022). This is demonstrated by first detections of vinylacetylene (C₂H₃CCH; Cernicharo et al. 2021a), vinylcyanoacetylene (C₂H₃C₃N; Lee et al. 2021), and vinylamine (C₂H₃NH₂; Zeng et al. 2021) as well as by observations of excited vibrational states (see, e.g., Belloche et al. 2013; López et al. 2014) and isotopic species (Müller et al. 2008) for vinylcyanide (C₂H₃CN): the first vinyl-bearing molecule found in the ISM (Gardner & Winnewisser 1975). Interstellar searches were reported for vinyl formate (C₂H₃OCHO; Alonso et al. 2016; Coutens et al. 2022), vinyl acetate (C₂H₃OC(O)CH₃; Kolesníková et al. 2015), vinyl mercaptan (C₂H₃SH; Martin-Drumel et al. 2019), vinylisocyanate (C₂H₃NCO; Rodríguez-Almeida et al. 2021; Vávra et al. 2022), acrylic acid (C₂H₃C(O)OH; Alonso et al. 2015; Calabrese et al. 2015; Coutens et al. 2022), acrylamide (C₂H₃C(O)NH₂; Kolesníková et al. 2022), and vinyl alcohol (C₂H₃OH; Melosso et al. 2019). The presence of the latter in the ISM, together with propenal (C₂H₃CHO), was announced in the past (Turner & Apponi 2001; Hollis et al. 2004) but it has been unambiguously confirmed very recently (Agúndez et al. 2021; Manigand et al. 2021).

An important part of this activity has concerned the role of isomers in the paradigm of interstellar chemistry (Green & Herbst 1979; Hollis 2005; Remijan et al. 2005). Vinyl moiety is present in some complex organic molecules (COMs; molecules with at least six atoms as defined in the astrochemical context by Herbst & van Dishoeck 2009), which exemplify members of families of isomer compounds with general formula C_xH_yO_z

(Karton & Talbi 2014). Mapping rotational transitions of isomer pairs acts as a fundamental tracer of processes controlling their formation and destruction, abundance ratio, or spatial distribution. This is shown through the observations and modeling of the C₂H₄O (Lykke et al. 2017), C₂H₄O₂ (Xue et al. 2019; Mininni et al. 2020), C₃H₂O (Loomis et al. 2015; Loison et al. 2016), C₃H₄O₂ (Coutens et al. 2022), and C₃H₆O₂ isomers (Lykke et al. 2017) among others (see, e.g., Cernicharo et al. 2020, 2021b; Shingledecker et al. 2020; Zhang et al. 2020). As COMs represent a sizable subset of interstellar species (Guélin & Cernicharo 2022; McGuire 2022), astronomical investigations of complex isomers help to elucidate one of the widely debated themes in astrochemistry: how chemical complexity and even prebiotic species build up in the ISM. Nevertheless, such investigations are critically dependent on the availability of laboratory data. Thus, as the variety and complexity of detected molecules rapidly increases, so does the importance of laboratory experiments to interpret new sensitive surveys. With this aim, two C₄H₈O isomers were recently studied by Sanz-Novo et al. (2022). Here, we focus on laboratory spectroscopy of vinylketene (C₂H₃CHCO), a representative of isomers with C₄H₄O empirical formula.

Ketenes, namely ketene (H₂CCO), methylketene (CH₃CHCO), and cyanoketene (NCCHCO), together with some related molecules such as propadienone (H₂CCCO) or ketenyl radical (HCCO) became targets of astronomical searches in the past. Ketene itself was detected toward Sgr B2 (Turner 1977) and other regions (Turner et al. 2020). Ketenyl radical was observed toward the starless core Lupus-1A and the molecular cloud L483 by Agúndez et al. (2015) while cyanoketene has not yet been detected (Margulès et al. 2020). Propadienone has also eluded detection so far (Loomis et al. 2015; Loison et al. 2016; Shingledecker et al. 2019), despite its two higher-energy isomers propynal (HCCCHO; Irvine et al. 1988) and cyclopropenone (c-C₃H₂O; Hollis et al. 2006) being found. Methylketene, the second most stable isomer in the C₃H₄O group, was searched for

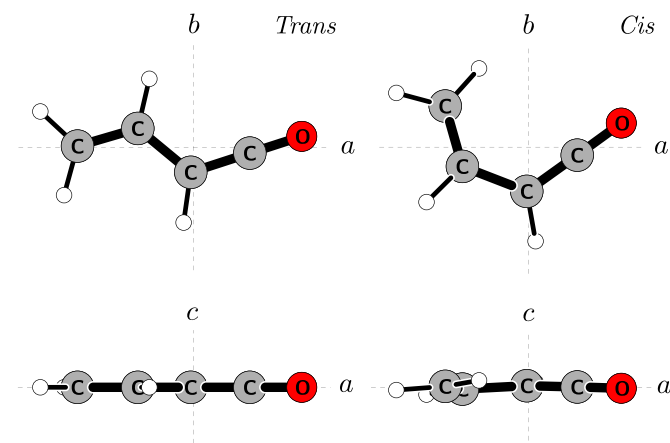


Figure 1. Optimized geometries of the two forms of vinylketene depicted in their ab and ac inertial planes.

in space using recent measurements in the millimeter wave domain (Bermúdez et al. 2018). Vinylketene also lies on the second position of the thermodynamic scale of the C_4H_4O isomers, right after furan ($c\text{-}C_4H_4O$; Lattalais et al. 2010). Attempts to detect furan have thus far been unsuccessful (Kutner et al. 1980; Dickens et al. 2001; Barnum et al. 2021, 2022). On the other hand, no searches were reported for vinylketene. This is likely due to the fact that, unlike furan (Barnum et al. 2021), laboratory data concerning the rotational transitions of this ketene derivative are rather scarce.

From the observational point of view, the most relevant target is the *trans* (or antiperiplanar) conformer (see Figure 1), which represents the most stable form of vinylketene. The second form, *cis* (or synperiplanar) conformer, is predicted by Badawi et al. (2001) to be less stable by 6.98 kJ mol^{-1} or 583 cm^{-1} or 840 K and, to the best of our knowledge, it has never been experimentally observed. The rotational spectrum of the *trans* species was first studied in 1979 independently by Bjarnov (1979) and Brown et al. (1979) using Stark modulation spectroscopy below 38 GHz. As usual, the analyses of low- J and $-K_a$ transitions rendered only limited sets of spectroscopic constants that pose difficulties in generating reliable predictions at millimeter wavelengths. Consequently, no spectral line catalog for vinylketene is publicly accessible to the astronomical community.

Here we report on significant improvements on all these aspects by measurements and analysis of the rotational spectrum of vinylketene in selected frequency regions up to 324 GHz. Similarly to our recent laboratory efforts on vinyl-bearing molecules such as acrylamide (Kolesníková et al. 2022) and vinylisocyanate (Vávra et al. 2022), we provide accurate rest frequencies of vinylketene to facilitate its search and eventual detection in the ISM.

2. Experimental Details

The experimental procedure consisted of three consecutive steps: synthesis of the precursor, in situ generation of vinylketene, and spectral measurements.

The synthesis of 3-butenic anhydride precursor has already been reported. Reaction of 3-butenic acid with dicyclohexylcarbodiimide (DCC; Brambilla et al. 1981; Oldroyd & Weedon 1994) or 3-butenyl chloride with 3-butenic acid sodium salt (Brown et al. 1979) gave the expected compound.

However, due to the presence of impurities in the first approach, we used oxalyl chloride and not DCC to synthesize the anhydride from the corresponding carboxylic acid. To a stirred solution under dry nitrogen of 3-butenic acid (8.6 g, 100 mmol) diluted in benzene (50 ml) was added dropwise oxalyl chloride (6.4 g, 51 mmol). The mixture was refluxed for 2 hr and then the low boiling point compounds were distilled under vacuum to a pressure of 0.1 mbar at room temperature. The yield was: 5.9 g, 77%.

3-Butenoic anhydride was thermolyzed in a quartz tube inserted in an oven heated to 430°C . The gaseous mixture emanating from the tube passed into a U-tube trap immersed in a bath at -50°C to eliminate the formed 3-butenic acid and the residual precursor. The thus purified flow containing almost pure vinylketene was continuously introduced into a 2.8 m long Pyrex glass free-space cell of the spectrometer at a pressure between 30 and $40 \mu\text{bar}$.

The rotational spectra were recorded using the upgraded Prague semiconductor millimeter wave spectrometer (Kania et al. 2006) over the frequency regions 195–218 and 292–324 GHz. These were reached by a multiplication ($8\times$ and $12\times$) of a fundamental synthesizer frequency by a set of active and passive multipliers. The optical path length was doubled using a roof-top mirror. The synthesizer output was modulated at the frequency $f = 28 \text{ kHz}$. The detection system consisted of zero-bias detectors and was completed by a demodulation procedure utilizing a lock-in amplifier with the time constant set to 20 ms. The lock-in amplifier was tuned to detect the signal at $2f$. The spectrum was obtained as an average of scans sweeping forwards and backwards in a single acquisition cycle. Assignment and Analysis of Broadband Spectra (AABS) package (Kisiel et al. 2005, 2012) was used for spectra processing and analyses.

3. Quantum-chemical Calculations

Badawi et al. (2001) reported equilibrium rotational constants for the *trans* and *cis* conformers of vinylketene at the B3LYP/6-311++G(d,p) level of theory. The nature of our experiment however requires to account for the vibrational corrections to rotational constants and molecular nonrigidity by means of reliable estimations of centrifugal distortion constants. To this end, we employed more expensive, but more sophisticated quantum-chemical calculations at the coupled-cluster-single-double (CCSD) level of theory (Purvis & Bartlett 1982) with Dunning’s Correlation-consistent triple- ζ (cc-pVTZ) basis set (Dunning 1989). The high-level rotational constants, quartic, and sextic centrifugal distortion constants have been determined by parallel algorithm on the basis of finite difference calculations of analytic gradients. All calculations have been carried out using the CFOUR program package (Matthews et al. 2020) and converged to 10^{-11} atomic units in energy, coupled-cluster amplitude equations, and Hartree–Fock self-consistent field equations.

4. Spectroscopic Analyses and Results

4.1. *Trans* Conformer

It can be appreciated from Figure 2 that the rotational spectrum of the *trans* species exhibits properties typical for a near-prolate asymmetric top with leading dipole moment component along the a principal inertial axis (see the dipole moment values in Table 1). Lines belonging to a -type R -branch

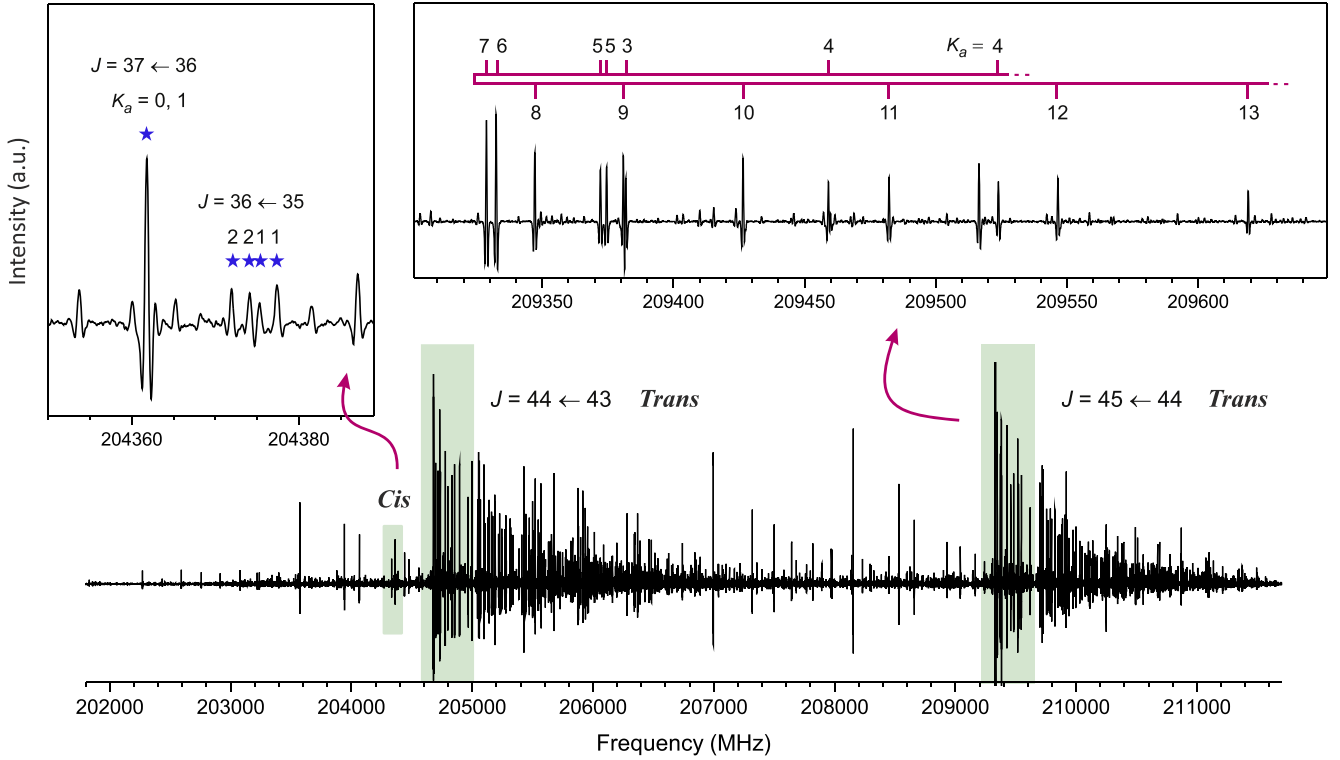


Figure 2. Section of the millimeter wave spectrum of vinylketene where two intense groups of a -type R -branch transitions are visible for the *trans* species. Those for the ground vibrational state are highlighted and one of them is unfolded in the upper right inset. Characteristic spectral features of the *cis* conformer are shown in the upper left inset. Here, weak a -type and b -type R -branch transitions between nearly degenerate pairs of levels with $K_a = 1, 2$ form a quartet in which the components are $36_{1,35} \leftarrow 35_{2,34}$, $36_{2,35} \leftarrow 35_{2,34}$, $36_{1,35} \leftarrow 35_{1,34}$, and $36_{2,35} \leftarrow 35_{1,34}$ in order of frequency. On the other hand, the four transitions originating from a pair of $K_a = 0, 1$ levels are collapsed into a single line.

transitions are predominant and at the scale of Figure 2 they form easily recognizable groups. We straightforwardly assigned the ground state a -type R -branch transitions up to $K_a = 9$ relying on previous microwave works (Bjarnov 1979; Brown et al. 1979) and our calculated centrifugal distortion constants from Table 1. At the highest-frequency end of our records we reached $J = 70$. The analysis, which employed Watson’s A -reduced sextic centrifugal distortion Hamiltonian (Watson 1977), allowed to predict and locate b -type transitions. Even though these transitions reach the confusion limit much sooner than a -type transitions, we managed to assign several series of b -type R -branch and Q -branch transitions and a few very weak b -type P -branch transitions. The subset of b -type transitions contained energy levels with J and K_a up to 89 and 9, respectively.

Attempts to analyze $K_a > 9$ transitions using sextic centrifugal distortion parameters resulted in a noticeable degradation of the fit. In particular, the observed minus calculated values became progressively worse in the higher-frequency region of our records and the higher K_a the lower J could be well fitted. We therefore present in Table 1 two fits. The Fit I encompasses transitions amenable to sextic centrifugal distortion Hamiltonian. As far as the standard deviation of the fit is concerned, the inclusion of two octic constants allowed to account for all transitions up to $K_a = 15$ and the Fit II reports the results for their most efficient combination. $K_a > 15$ transitions were also observed but were not further taken into consideration due to even larger departures with respect to their predicted positions.

The issues associated with difficulties to fit the high- K_a transitions are further discussed in Section 5. For completeness, Watson’s S -reduced Hamiltonian was also tested and led to results of very similar quality.

The complete list of analyzed transitions is provided in Table A1. We note that microwave transitions only from Bjarnov (1979) are included in this list as the data set from Brown et al. (1979) showed deviations. We observed that when data from Brown et al. (1979) are analyzed separately, a reasonable fit can be obtained with the results given in Table 1. However, when these data are merged with our data set and that from Bjarnov (1979), systematic deviations up to 300 kHz appeared almost for all transitions from Brown et al. (1979) while those from Bjarnov (1979) fit perfectly. A difference in the microwave data can be already seen by comparing frequencies of common transitions. For example, the transition $5_{1,5} \leftarrow 4_{1,4}$ was measured by Bjarnov (1979) at 22900.870 MHz while Brown et al. (1979) reported 22900.633 MHz. For this reason, we preferred not to include the rotational transitions from Brown et al. (1979) into the global analysis.

Finally, rotational (Q_{rot}) and vibrational (Q_{vib}) partition functions at seven different temperatures are provided in Table 2. The former was obtained by numerical summation over the levels up to $J = 245$ and $K_a = 59$ using the SPCAT program (Pickett 1991) and the results from Fit I. The vibrational partition function was obtained using the Equation (3.60) of Gordy & Cook (1970) assuming the anharmonic frequencies of normal vibrational modes from Table A2.

Table 1
Spectroscopic Constants of *trans* Vinylketene (A-reduced Hamiltonian, I^r-representation)

			Experimental ^a		Calculated ^c
	Fit I	Fit II	Bjarnov (1979)	Brown et al. (1979) ^b	
A_0/MHz	39532.8065 (14)	39532.8254 (15)	39571 (48)	39560 (24)	39560.15
B_0/MHz	2392.93788 (12)	2392.93739 (11)	2392.9252 (28)	2392.9048 (28)	2385.30
C_0/MHz	2255.99521 (10)	2255.99468 (10)	2256.0089 (28)	2255.9947 (26)	2249.32
Δ_J/kHz	0.404404 (34)	0.404264 (32)	0.414 (31)	0.505 (18)	0.3785
Δ_{JK}/kHz	-34.66747 (65)	-34.65355 (70)	-34.694 (92)	-34.785 (38)	-32.72
Δ_K/kHz	1651.624 (62)	1652.335 (63)	1568
δ_J/kHz	0.0550371 (46)	0.0550400 (46)	0.05153
δ_K/kHz	3.8176 (26)	3.8201 (25)	2.932
Φ_J/mHz	0.5356 (32)	0.5237 (31)	0.4650
Φ_{JK}/mHz	-61.12 (49)	-58.33 (47)	-56.10
Φ_{KJ}/Hz	1.6962 (57)	2.1362 (82)	1.498
Φ_K/Hz	34.24 (68)	36.91 (67)	36.98
ϕ_J/mHz	0.14564 (48)	0.14602 (48)	0.1316
ϕ_{JK}/mHz	7.40(40)	7.34 (40)	4.275
ϕ_K/Hz	6.84 (17)	7.29 (17)	6.004
L_{JK}/mHz	...	-0.04108 (65)
L_{KKJ}/mHz	...	-1.510 (28)
$ \mu_a /\text{D}$	0.865 (14)	0.872 (1)	0.79
$ \mu_b /\text{D}$	0.475 (41)	0.416 (57)	0.44
$ \mu_c /\text{D}$	0.00
J_{\min}/J_{\max}	1/89	1/89	1/6	2/8	...
K_a^{\min}/K_a^{\max}	0/12 ^d	0/15	0/5	0/7	...
N^e	330	378	28	28	...
$\sigma_{\text{fit}}^f/\text{MHz}$	0.020	0.021	0.0265	0.035	...
σ_w^g	0.88	0.95	...	1.00	...

Notes.

^a The numbers in parentheses are the parameter uncertainties in units of the last decimal digits. Their values are close to 1σ standard uncertainties because the unitless (weighted) deviation of the fit is close to 1.0. SPFIT/SPCAT program package (Pickett 1991) was used for the analysis.

^b Obtained by refitting the microwave transitions using the same Hamiltonian model as in this work.

^c Calculated at CCSD/cc-pVTZ level of theory.

^d $K_a = 10$ – 12 only up to $J = 46$.

^e Number of distinct frequency lines in the fit.

^f Rms deviation of the fit.

^g Unitless (weighted) deviation of the fit.

Table 2Rotational and Vibrational Partition Functions for *trans* Vinylketene

T (K)	Q_{rot}	Q_{vib}
300.000	60251.16	6.50
225.000	39089.70	3.43
150.000	21254.51	1.91
75.000	7507.66	1.16
37.500	2654.10	1.01 ^c
18.750	939.00	1.00
9.375	332.58	1.00

4.2. Cis Conformer

While the quantum-chemical calculations of the lowest-energy conformer passed smoothly and resulted in a planar structure with C_s symmetry, a prediction of the structure of the *cis* conformer was not straightforward. Contrary to the previous computational study (Badawi et al. 2001), which presented a planar structure as a local minimum at the DFT/B3LYP/6-311++G(d,p) level of theory, we found it as a transition state using CCSD/cc-pVTZ calculations. The frequency analysis performed within the planar structure detected a single very soft imaginary mode ($\nu_{21} = i25 \text{ cm}^{-1}$). This mode corresponds

to a torsion about the C–C bond and it involves changes only in dihedral angles. The scan of potential energy curve along this imaginary normal mode is displayed in Figure 3. It has been done by multiplying the value of the normal mode vector with all other coordinates kept frozen. When a minimum was found, all coordinates have been optimized (see the blue diamonds in the Figure 3). The planar structure corresponds to the transition state between two symmetrically equivalent nonplanar structures belonging to C_1 symmetry point group. Two sets of the calculated spectroscopic constants are thus collected in Table 3: for the planar transition state (C_s symmetry) and for the local minimum (C_1 symmetry). Although a single imaginary frequency was obtained within the planar C_s structure, this structure has an optimized geometry and is in a sense a stable conformation. It means the calculated centrifugal distortion constants (and the other vibrational-rotational constants) have physical meaning and they are valid for this structure (Miller et al. 1990).

The observation of line grouping or other specific patterns is extremely useful in searches and assignment of the spectrum of a new species. Regardless of whether the molecular structure of the *cis* conformer is planar or slightly nonplanar, it is a prolate asymmetric rotor with relevant dipole moment components

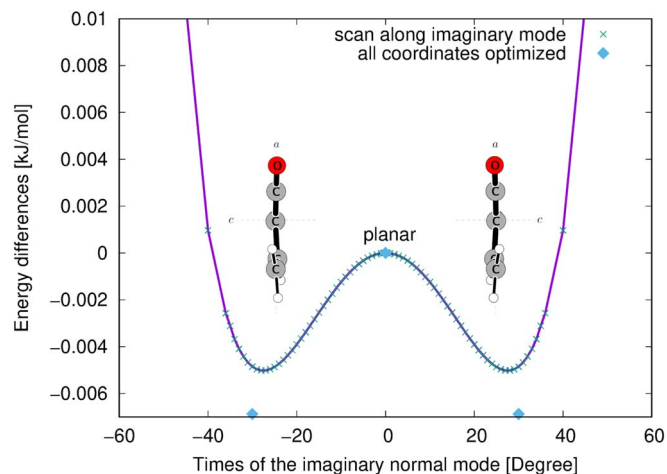


Figure 3. Potential energy scan along the imaginary normal mode ν_{21} undertaken within the CCSD/cc-pVTZ level of theory. The optimized energies of the planar and two slightly nonplanar symmetrically equivalent structures are denoted by blue diamond points.

along the a and b inertial axes (see Table 3). For certain values of J and K_a this should lead to the observations of quartets consisting of an inner pair of a -type transitions and an outer pair of b -type transitions such as those found in the spectra of lactic acid (Pszczółkowski et al. 2005) or the higher-energy conformer of acrylamide (Kolesníková et al. 2022). It was eventually possible to locate candidate lines among the many unassigned lines of the *trans* conformer. One of the identified quartets is exemplified in Figure 2. Since the pertinent lines were weak, Loomis–Wood-type plots from the AABS package (Kisiel et al. 2005, 2012) were invaluable in assisting the analysis and avoiding misassignments.

We finally assigned rotational transitions with J values spanning from 8 to 61 and K_a values from 0 to 24. This data set includes a -type R -branch transitions as well as b -type R -branch and Q -branch transitions and is listed in Table A3. Watson’s A -reduced Hamiltonian (Watson 1977) with all terms up to the sixth power in angular momentum was used to fit these transitions and the result is shown in Table 3.

5. Discussion

Table 1 compares parameters obtained for *trans* vinylketene with those determined previously and those from harmonic and anharmonic force field calculations at CCSD/cc-pVTZ level of theory. We find an agreement between our constants and those from Bjarnov (1979) as well as Brown et al. (1979) and, more importantly, we find a significant improvement in their values. For example, the rotational constant A has been improved by several orders of magnitude thanks to the measurements of b -type transitions, which were not observed in previous studies. In addition, the vast majority of centrifugal distortion constants is determined for the first time.

If we are more interested in physical meaning of values of each of the parameters used, then the Fit I would be the choice. On the other hand, if the predictive power of higher- K_a transitions is the purpose, then the Fit II is preferable. The Fit II encompasses more $K_a > 9$ transitions; however, values of the obtained constants are likely affected by rovibrational interactions with low-lying excited vibrational states. According to our quantum-chemical calculations, the lowest excited

Table 3
Spectroscopic Constants of *cis* Vinylketene (A -reduced Hamiltonian, I^r -representation)

	Experimental ^b	Calculated ^a	
		C_s	C_1
A_0 /MHz	13853.6798 (17)	14036.22 ^c	13935.24
B_0 /MHz	3396.41708 (53)	3363.12 ^c	3382.30
C_0 /MHz	2728.40289 (48)	2713.07 ^c	2682.57
Δ_J /kHz	3.28512 (20)	3.004	3.103
Δ_{JK} /kHz	−33.28989 (82)	−31.32	−31.02
Δ_K /kHz	140.449 (14)	135.8	136.7
δ_J /kHz	1.00508 (12)	0.9076	0.9299
δ_K /kHz	8.0002 (68)	6.930	10.28
Φ_J /mHz	12.991 (42)	11.27	12.21
Φ_{JK} /mHz	−24.0 (16)	−41.27	37.52
Φ_{KJ} /Hz	−0.9324 (60)	−0.8801	−1.634
Φ_K /Hz	4.755 (35)	4.935	4.575
ϕ_J /mHz	5.784 (23)	4.939	5.436
ϕ_{JK} /mHz	32.7 (17)	19.03	40.25
ϕ_K /Hz	1.971 (40)	1.592	5.841
$ \mu_a /D$...	0.71	0.73
$ \mu_b /D$...	1.04	1.04
$ \mu_c /D$...	0.00	0.02
J_{\min}/J_{\max}	8/61
K_a^{\min}/K_a^{\max}	0/24
N^d	263
σ_{fit}^e /MHz	0.027
σ_w^f	0.95

Notes.

^a Calculated at CCSD/cc-pVTZ level of theory.

^b The numbers in parentheses are the parameter uncertainties in units of the last decimal digits. Their values are close to 1σ standard uncertainties because the unitless (weighted) deviation of the fit is close to 1.0. SPFIT/SPCAT program package (Pickett 1991) was used for the analysis.

^c Equilibrium values because the C_s structure is not a local minimum.

^d Number of distinct frequency lines in the fit.

^e Rms deviation of the fit.

^f Unitless (weighted) deviation of the fit.

vibrational state, namely $\nu_{21} = 1$, is located around 117 cm^{-1} . Due to the large value of the A rotational constant, rovibrational interactions might appear already for relatively low values of K_a quantum numbers. A similar situation has been observed for *trans* vinylisocyanate (Vávra et al. 2022) and other near-prolate species such as vinylcyanide (Kisiel et al. 2009, 2012). For *trans* vinylisocyanate, only transitions involving levels up to $K_a = 6$ could be analyzed without the loss of physical meaning of the fitted constants (Vávra et al. 2022). In the present case, the A rotational constant is smaller and the lowest excited vibrational state lies higher in energy than in *trans* vinylisocyanate so levels up to $K_a = 9$ are expected to be free from interactions within the covered range of J quantum numbers and thus serve as an accurate observational reference.

Spectroscopic parameters obtained for the less stable *cis* conformer are provided in Table 3. They comprise the rotational constants and full sets of quartic and sextic centrifugal distortion constants and rely on the observations of a -type and b -type transitions. No c -type transitions were found in the spectrum. This points to the planar structure of the species, nevertheless a slightly nonplanar structure cannot be completely ruled out as the predicted dipole moment along the c axis is very small (see Table 3). In addition, if tunneling

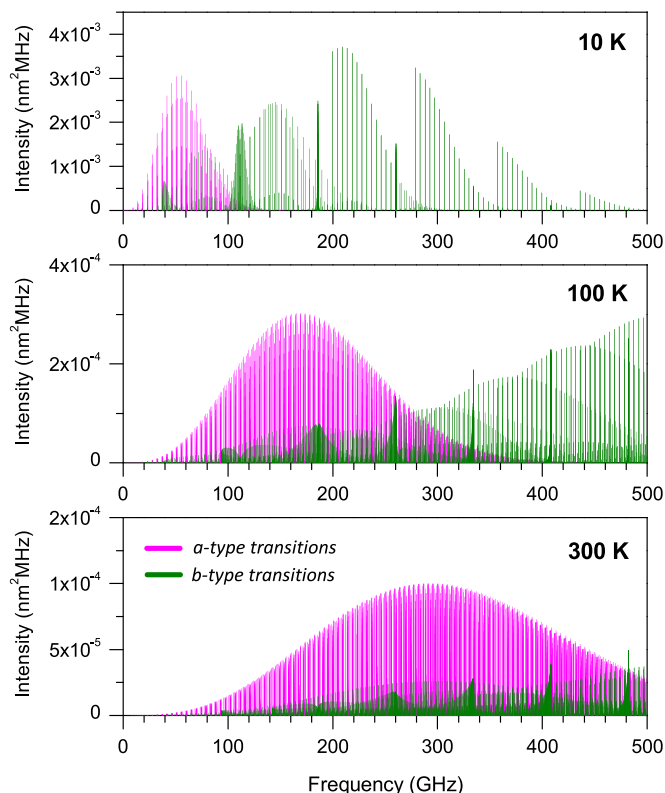


Figure 4. Temperature dependence distribution of the rotational spectrum of *trans* vinylketene.

between two symmetry equivalent structures of the molecule existed, these would be observable between the resulting pair of states. We however note that no signs for such tunneling have been unambiguously observed in our spectrum. Another evidence about the molecular planarity comes from the value of the inertial defect, which is zero for a strictly planar and rigid molecule. In the present case, the small and negative value $\Delta = -0.049 \text{ u}\text{\AA}^2$ shows that the species is planar with a zero-point contribution from out-of-plane vibrations (Oka 1995). Similar values were found, for instance, for acrylic acid ($-0.049 \text{ u}\text{\AA}^2$ and $-0.051 \text{ u}\text{\AA}^2$ for the *trans* and *cis* conformer, respectively, Bolton et al. 1968) and *s-trans*-1,3-butadiene-1,1- d_2 ($-0.0256 \text{ u}\text{\AA}^2$, Caminati et al. 1988), which are also considered planar. These observations are not in disagreement with our quantum-chemical calculations, which indicated a nonplanar C_1 structure as the global minimum of the *cis* conformer because the calculated energy barrier to the planarity is very low ($0.0069 \text{ kJ mol}^{-1}$ or 0.577 cm^{-1}). Considering the zero-point vibrational energy, the structure of the molecule can be viewed as effectively planar. An overview of the results in Table 3 further supports this suggested planarity statement. The set of calculated spectroscopic constants for the planar transition state is in better agreement with its experimental counterpart than that for the nonplanar structure.

6. Spectral Predictions

A graphical representation of the pure rotational spectrum of *trans* vinylketene at 10, 100, and 300 K is shown in Figure 4. The higher-frequency region covered in this work is just beyond the absorption maximum at 300 K, so that the lines most likely to be detected in the interstellar medium are well characterized. We did not measure the continuous spectrum up

to 324 GHz, nevertheless, the inclusion of low- J transitions from Bjarnov (1979) makes confident the interpolated predictions. We examined the quality of our analysis and predictions by removing the transitions from Bjarnov (1979). No significant effect on the fit has been observed and the rotational transitions from Bjarnov (1979) could be perfectly predicted. Consequently, rotational transitions showing nonnegligible deviations from Brown et al. (1979; see Section 4) are also expected to be accurately predicted.

To assist searches for vinylketene in the ISM, we provide a list of frequency predictions for the *trans* conformer in Table A4. The key parameters used in the generation of this table are: $\mu_a = 0.865 \text{ D}$ and $\mu_b = 0.475 \text{ D}$ taken from Bjarnov (1979), $T = 300 \text{ K}$, and $Q_{\text{rot}} = 60251.1579$. The predictions are truncated at $K_a = 9$ due to rovibrational interactions discussed in Section 5. We note that due to the large value of the A rotational constant, $K_a = 9$ is more than sufficient to detect the molecule in warm environments such as hot cores as well as in cold regions. Nevertheless, if needed, predictions for $K_a > 9$ transitions are available from the authors. These are, however, advised to be checked against experimentally measured frequencies from Table A1 due to possible perturbations in the spectrum.

7. Concluding Remarks

A new laboratory study of the rotational spectrum of vinylketene has been undertaken in selected frequency regions up to 324 GHz and was accompanied by high-level quantum-chemical calculations relying on coupled-cluster methods. Over 300 transition lines were assigned and measured for *trans* vinylketene and values of its spectroscopic parameters with an accuracy conducive to a reliable interstellar search were obtained. In addition, the first experimental evidence for the less stable *cis* conformer is reported by means of 263 rotational lines. Their analysis provided the first set of molecular constants for the *cis* species and complements the spectroscopic characterization of vinylketene.

Understanding of how COMs and possible related prebiotic molecules form in the ISM represents one of the major topics in the field of astrochemistry and astrobiology. A significant amount of isomers among COMs motivates for astronomical investigations of different families of isomer compounds. This work creates an excellent opportunity for interstellar probing of C_4H_4O isomers by means of a catalog of accurate frequencies and intensities for the lowest-energy conformer of vinylketene over a wide frequency range.

This work has been funded by the Czech Science Foundation (GACR, grant No. 19-25116Y). L.K., J.K., and K.L. gratefully acknowledge this financial support. L.K., J.K., K.L., and P.K. thank the financial support from the Ministry of Education, Youth and Sports of the Czech Republic (MSMT) within the Mobility grant No. 8J21FR006. Computational resources were supplied by the project “e-Infrastruktura CZ” (e-INFRA CZ LM2018140) supported by the Ministry of Education, Youth and Sports of the Czech Republic. Computational resources were provided by the ELIXIR-CZ project (LM2018131), part of the international ELIXIR infrastructure. J.-C.G. thanks the Centre National d’Etudes Spatiales (CNES) and the “Programme National Physique et Chimie du Milieu Interstellaire” (PCMI) of CNRS/INSU with INC/INP cofunded by CEA and CNES for a grant.

Appendix Complementary Tables

Tables A1 and A2 list the measured transitions and the frequencies of normal vibrational modes of *trans* vinylketene,

respectively. Table A3 lists the measured transitions of *cis* vinylketene and Table A4 lists the JPL/CDMS line catalog for *trans* vinylketene.

Table A1
List of Measured Transitions of *trans* Vinylketene

J'	K'_a	K'_c	J''	K''_a	K''_c	$\nu_{\text{obs}}^{\text{a}}$ (MHz)	$u_{\text{obs}}^{\text{b}}$ (MHz)	Fit I		Fit II		Weight ^e	Notes ^f
								$\nu_{\text{obs}} - \nu_{\text{calc}}^{\text{c}}$ (MHz)	$(\nu_{\text{obs}} - \nu_{\text{calc}})^{\text{d}}$ (MHz)	$\nu_{\text{obs}} - \nu_{\text{calc}}$ (MHz)	$(\nu_{\text{obs}} - \nu_{\text{calc}})^{\text{b}}$ (MHz)		
2	0	2	1	0	1	9297.4740	0.025	-0.0013	...	0.0006	(1)
4	1	4	3	1	3	18321.3150	0.025	0.0030	...	0.0072	(1)
44	6	38	43	6	37	204679.9894	0.020	-0.0221	-0.0015	-0.0143	0.0063	0.50	(2)
44	6	39	43	6	38	204679.9894	0.020	0.0190	-0.0015	0.0268	0.0063	0.50	(2)
65	1	65	64	1	64	295181.4961	0.020	0.0009	...	-0.0042	(2)
69	2	68	68	2	67	317356.1450	0.020	0.0022	...	-0.0020	(2)
68	13	55	67	13	54	316530.5079	0.020	0.0130	0.0130	0.50	(2)
68	13	56	67	13	55	316530.5079	0.020	0.0130	0.0130	0.50	(2)

Notes.

^a Observed frequency.

^b Uncertainty of the observed frequency.

^c Observed minus calculated frequency.

^d Observed minus calculated frequency for blends.

^e Intensity weighting factor for blended transitions.

^f Data source: (1) Bjarnov (1979), (2) This work.

(This table is available in its entirety in machine-readable form.)

Table A2
Frequencies of Normal Vibrational Modes for *trans* Vinylketene Calculated at CCSD/cc-pVTZ Level of Theory

Mode	Harmonic Freq. (cm^{-1})	Anharmonic Freq. (cm^{-1})	Symmetry
1	3267.1	3125.1	A'
2	3235.1	3102.7	A'
3	3191.6	3047.3	A'
4	3173.4	3041.2	A'
5	2222.7	2180.1	A'
6	1714.8	1670.8	A'
7	1496.6	1457.4	A'
8	1377.2	1357.6	A'
9	1333.1	1310.9	A'
10	1198.0	1174.3	A'
11	1131.3	1125.9	A'
12	935.9	923.2	A'
13	639.1	629.6	A'
14	410.5	412.4	A'
15	169.5	169.6	A'
16	1022.6	998.9	A''
17	914.5	900.0	A''
18	712.0	699.1	A''
19	556.6	547.9	A''
20	531.4	523.7	A''
21	119.8	116.9	A''

Table A3
List of Measured Transitions of *cis* Vinylketene

J'	K'_a	K'_c	J''	K''_a	K''_c	ν_{obs}^a (MHz)	$\nu_{\text{obs}} - \nu_{\text{calc}}^b$ (MHz)	u_{obs}^c (MHz)	$(\nu_{\text{obs}} - \nu_{\text{calc}})^b_d$ (MHz)	Weight ^e
38	1	37	37	2	36	215238.6354	0.0111	0.020
36	2	34	35	2	33	209902.1709	-0.0113	0.030
52	3	49	51	4	48	302056.6935	-0.0071	0.025
34	5	30	33	5	29	209142.1707	0.0236	0.030
35	11	24	34	11	23	216095.3853	-0.0353	0.030	-0.0029	0.50
35	11	25	34	11	24	216095.3853	0.0294	0.030	-0.0029	0.50

Notes.^a Observed frequency.^b Observed minus calculated frequency.^c Uncertainty of the observed frequency.^d Observed minus calculated frequency for blends.^e Intensity weighting factor for blended transitions.

(This table is available in its entirety in machine-readable form.)

Table A4
Jet Propulsion Laboratory (JPL)/CDMS Catalog Line List for *trans* Vinylketene

ν_{calc}^a (MHz)	u_{calc}^b (MHz)	Log(Int) ^c	DR ^d	E_{low}^e (cm ⁻¹)	g_{upp}^f	TAG ^g	QNFMT ^h	J'	K'_a	K'_c	J''	K''_a	K''_c
4648.9315	0.0002	-8.7480	3	0.0000	3	68512	303	1	0	1	0	0	0
6987.8982	0.0029	-8.3053	3	6.7409	19	68512	303	9	0	9	8	1	8
8311.3827	0.0023	-8.3619	3	3.2556	11	68512	303	5	1	5	6	0	6
9161.0663	0.0004	-7.9858	3	1.3939	5	68512	303	2	1	2	1	1	1
9297.4754	0.0004	-7.8454	3	0.1551	5	68512	303	2	0	2	1	0	1
9408.7676	0.0080	-8.1291	3	241.9614	109	68512	303	54	3	51	53	4	50
9434.9176	0.0004	-7.9602	3	1.3984	5	68512	303	2	1	1	1	1	0

Notes.^a Predicted frequency.^b Predicted uncertainty of the frequency.^c Base 10 logarithm of the integrated intensity at 300 K in units of nm² MHz.^d Degrees of freedom in the rotational partition function.^e Lower state energy.^f Upper state degeneracy.^g Species tag or molecular identifier.^h Format of the quantum numbers. This table is available in its entirety in machine-readable form but the data portion still follows the JPL/CDMS catalog format.

(This table is available in its entirety in machine-readable form.)

ORCID iDsLucie Kolesníková  <https://orcid.org/0000-0003-3567-0349>Tereza Uhlíková  <https://orcid.org/0000-0002-6220-2092>Jan Koucký  <https://orcid.org/0000-0001-9498-9400>Kateřina Luková  <https://orcid.org/0000-0002-0087-0626>Patrik Kania  <https://orcid.org/0000-0001-8338-3569>Jean-Claude Guillemin  <https://orcid.org/0000-0002-2929-057X>Štěpán Urban  <https://orcid.org/0000-0002-4566-4930>**References**

Agúndez, M., Cernicharo, J., & Guélin, M. 2015, *A&A*, **577**, L5
 Agúndez, M., Marcelino, N., Tercero, B., et al. 2021, *A&A*, **649**, L4
 Alonso, E. R., Kolesníková, L., Peña, I., et al. 2015, *JMoSp*, **316**, 84
 Alonso, E. R., Kolesníková, L., Tercero, B., et al. 2016, *ApJ*, **832**, 42
 Badawi, H., Förner, W., & Al-Saadi, A. 2001, *JMoSt*, **535**, 183
 Barnum, T. J., Lee, K. L. K., & McGuire, B. A. 2021, *ESC*, **5**, 2986
 Barnum, T. J., Siebert, M. A., Lee, K. L. K., et al. 2022, *JPCA*, **126**, 2716
 Belloche, A., Müller, H. S. P., Menten, K. M., Schilke, P., & Comito, C. 2013, *A&A*, **559**, A47

Bermúdez, C., Tercero, B., Motiyenko, R. A., et al. 2018, *A&A*, **619**, A92
 Bjamov, E. 1979, *ZNatA*, **34**, 1269
 Bolton, K., Owen, N. L., & Sheridan, J. 1968, *Natur*, **218**, 266
 Brambilla, R., Friary, R., Ganguly, A., et al. 1981, *Tetrahedron*, **37**, 3615
 Brown, R. D., Godfrey, P. D., & Woodruff, M. 1979, *AJCh*, **32**, 2103
 Calabrese, C., Maris, A., Dore, L., et al. 2015, *MolPh*, **113**, 2290
 Caminati, W., Grassi, G., & Bauder, A. 1988, *CPL*, **148**, 13
 Cernicharo, J., Agúndez, M., Cabezas, C., et al. 2021a, *A&A*, **647**, L2
 Cernicharo, J., Agúndez, M., Kaiser, R. I., et al. 2021b, *A&A*, **655**, L1
 Cernicharo, J., Marcelino, N., Agúndez, M., et al. 2020, *A&A*, **642**, L8
 Coutens, A., Loison, J.-C., Boulanger, A., et al. 2022, *A&A*, **660**, L6
 Dickens, J., Irvine, W., Nummelin, A., et al. 2001, *AcSpA*, **57**, 643
 Dunning, T. H. 1989, *JChPh*, **90**, 1007
 Gardner, F. F., & Winnewisser, G. 1975, *ApJL*, **195**, L127
 Gordy, W., & Cook, R. L. 1970, *Microwave Molecular Spectra* (New York: Interscience)
 Green, S., & Herbst, E. 1979, *ApJ*, **229**, 121
 Guélin, M., & Cernicharo, J. 2022, *FrASS*, **9**, 787567
 Herbst, E., & van Dishoeck, E. F. 2009, *ARA&A*, **47**, 427
 Hollis, J. M. 2005, in *IAU Symp. 231, Astrochemistry: Recent Successes and Current Challenges* (Cambridge: Cambridge Univ. Press), 227
 Hollis, J. M., Jewell, P. R., Lovas, F. J., Remijan, A., & Møllendal, H. 2004, *ApJL*, **610**, L21
 Hollis, J. M., Remijan, A. J., Jewell, P. R., & Lovas, F. J. 2006, *ApJ*, **642**, 933

- Irvine, W. M., Brown, R. D., Cragg, D. M., et al. 1988, *ApJL*, 335, L89
- Kania, P., Štríteská, L., Šimečková, M., & Urban, Š. 2006, *JMoSt*, 795, 209
- Karton, A., & Talbi, D. 2014, *CP*, 436, 22
- Kisiel, Z., Pszczółkowski, L., Drouin, B. J., et al. 2009, *JMoSp*, 258, 26
- Kisiel, Z., Pszczółkowski, L., Drouin, B. J., et al. 2012, *JMoSp*, 280, 134
- Kisiel, Z., Pszczółkowski, L., Medvedev, I. R., et al. 2005, *JMoSp*, 233, 231
- Kolesníková, L., Belloche, A., Koucký, J., et al. 2022, *A&A*, 659, A111
- Kolesníková, L., Peña, I., Alonso, J. L., et al. 2015, *A&A*, 577, A91
- Kutner, M. L., Machnik, D. E., Tucker, K. D., & Dickman, R. L. 1980, *ApJ*, 242, 541
- Lattalais, M., Ellinger, Y., Matrane, A., & Guillemin, J.-C. 2010, *PCCP*, 12, 4165
- Lee, K. L. K., Loomis, R. A., Burkhardt, A. M., et al. 2021, *ApJL*, 908, L11
- Loison, J.-C., Agúndez, M., Marcelino, N., et al. 2016, *MNRAS*, 456, 4101
- Loomis, R. A., McGuire, B. A., Shingledecker, C., et al. 2015, *ApJ*, 799, 34
- López, A., Tercero, B., Kisiel, Z., et al. 2014, *A&A*, 572, A44
- Lykke, J. M., Coutens, A., Jørgensen, J. K., et al. 2017, *A&A*, 597, A53
- Manigand, S., Coutens, A., Loison, J.-C., et al. 2021, *A&A*, 645, A53
- Margulès, L., McGuire, B. A., Motiyenko, R. A., et al. 2020, *A&A*, 638, A3
- Martin-Drumel, M.-A., Lee, K. L. K., Belloche, A., et al. 2019, *A&A*, 623, A167
- Matthews, D. A., Cheng, L., Harding, M. E., et al. 2020, *JChPh*, 152, 214108
- McGuire, B. A. 2022, *ApJS*, 259, 30
- Melosso, M., McGuire, B. A., Tamassia, F., Degli Esposti, C., & Dore, L. 2019, *ESC*, 3, 1189
- Miller, W. H., Hernandez, R., Handy, N. C., Jayatilaka, D., & Willetts, A. 1990, *CPL*, 172, 62
- Mininni, C., Beltrán, M. T., Rivilla, V. M., et al. 2020, *A&A*, 644, A84
- Molpeceres, G., & Rivilla, V. M. 2022, *A&A*, 665, A27
- Müller, H. S., Belloche, A., Menten, K. M., Comito, C., & Schilke, P. 2008, *JMoSp*, 251, 319
- Oka, T. 1995, *JMoSt*, 352–353, 225
- Oldroyd, D. L., & Weedon, A. C. 1994, *J. Org. Chem.*, 59, 1333
- Pickett, H. M. 1991, *JMoSp*, 148, 371
- Pszczółkowski, L., Białkowska-Jaworska, E., & Kisiel, Z. 2005, *JMoSp*, 234, 106
- Purvis, G. D., & Bartlett, R. J. 1982, *JChPh*, 76, 1910
- Remijan, A. J., Hollis, J. M., Lovas, F. J., Plusquellic, D. F., & Jewell, P. R. 2005, *ApJ*, 632, 333
- Rodríguez-Almeida, L. F., Rivilla, V. M., Jiménez-Serra, I., et al. 2021, *A&A*, 654, L1
- Sanz-Novo, M., Belloche, A., Rivilla, V. M., et al. 2022, *A&A*, 666, A114
- Shingledecker, C. N., Álvarez-Barcia, S., Korn, V. H., & Kästner, J. 2019, *ApJ*, 878, 80
- Shingledecker, C. N., Molpeceres, G., Rivilla, V. M., Majumdar, L., & Kästner, J. 2020, *ApJ*, 897, 158
- Turner, A. M., Koutsogiannis, A. S., Kleimeier, N. F., et al. 2020, *ApJ*, 896, 88
- Turner, B. E. 1977, *ApJL*, 213, L75
- Turner, B. E., & Apponi, A. J. 2001, *ApJL*, 561, L207
- Vávra, K., Kolesníková, L., Belloche, A., et al. 2022, *A&A*, 666, A50
- Watson, J. K. G. 1977, in *Vibrational Spectra and Structure*, Vol. 6 ed. J. R. Durig (Amsterdam: Elsevier), 1
- Xue, C., Remijan, A. J., Burkhardt, A. M., & Herbst, E. 2019, *ApJ*, 871, 112
- Zeng, S., Jiménez-Serra, I., Rivilla, V. M., et al. 2021, *ApJL*, 920, L27
- Zhang, X., Quan, D., Chang, Q., et al. 2020, *MNRAS*, 497, 609